8-21-2008

Photoelectron spectroscopic and theoretical studies of Fem – (coronene)n (m=1,2, n=1,2) complexes

Xiang Li
Johns Hopkins University

Soren Eustis
Johns Hopkins University

Kit H. Bowen
Johns Hopkins University

Anil K. Kandalam
West Chester University of Pennsylvania, akandalam@wcupa.edu

Puru Jena
Virginia Commonwealth University

Recommended Citation

Li, X., Eustis, S., Bowen, K. H., Kandalam, A. K., & Jena, P. (2008). Photoelectron spectroscopic and theoretical studies of Fem – (coronene)n (m=1,2, n=1,2) complexes. *Journal of Chemical Physics, 129*(7), 074308-1-074308-11. http://dx.doi.org/10.1063/1.2968609

Photoelectron spectroscopic and theoretical studies of $Fe_m^-(coronene)_n$ ($m=1,2$, $n=1,2$) complexes

Xiang Li,[1] Soren Eustis,[1] Kit H. Bowen,[1,a),b)] Anil K. Kandalam,[2,a),c)] and Puru Jena[2]
[1]*Department of Chemistry and Department of Materials Science, Johns Hopkins University, Baltimore, Maryland 21218, USA*
[2]*Physics Department, Virginia Commonwealth University, Richmond, Virginia 23284, USA*

(Received 19 May 2008; accepted 16 July 2008; published online 21 August 2008)

$Fe_m(coronene)_n$ ($m=1,2$, $n=1,2$) cluster anions were generated by a laser vaporization source and studied by anion photoelectron spectroscopy. Density functional theory was used to calculate the structures and the spin multiplicities of those clusters as well as the electron affinities and photodetachment transitions. The calculated magnetic moments of $Fe_1(coronene)_1$ and $Fe_2(coronene)_1$ clusters suggest that coronene could be a suitable template on which to deposit small iron clusters and that these in turn might form the basis of an iron cluster-based magnetic material. $Fe_1(coronene)_2$ and $Fe_2(coronene)_2$ cluster anions and their corresponding neutrals prefer the sandwich-type structures, and the ground state structures of these clusters are all staggered sandwiches. © *2008 American Institute of Physics*. [DOI: 10.1063/1.2968609]

INTRODUCTION

The field of organometallic chemistry has made important contributions to the understanding of chemical interactions and has produced many compounds, which find widespread use in society. The development of laser vaporization techniques has extended the range of gas phase studies of the interaction between metal and organic ligands, further developing our understanding of the delicate and complex interactions present in organometallic complexes. Many experimental[1–12] and theoretical studies[13–17] have been reported on transition metal (TM)-benzene systems, including their corresponding anions and cations. These studies showed that TM-benzene clusters could form either a sandwich structure (Si, Ti, and V) or a so-called "rice-ball"—metal cluster core covered by benzene molecules—structure (Fe, Co, and Ni). Such studies also provided structural and electronic information about the clusters, thus building a basic model for understanding the interaction between the *d* electrons of transition metals and the π orbitals of organic molecules.

In addition, studies of the magnetic properties of the TM-organic complexes are important both with regard to the design and synthesis of novel magnetic materials and for developing a better understanding of magnetism in general. It is known from molecular beam deflection experiments[18–27] that bare clusters of iron, cobalt, and nickel possess large magnetic moments and that the per-atom moment for smaller size ($n<100$) clusters are considerably higher than those displayed by the corresponding bulk material.[28–31] The magnetic moment reaches a maximum at the atom in these cases. For instance, in the Fe atom ($3d^64s^2$), Hund's rule requires the total spin to be maximized; thus five of the $3d$ electrons fill to the $3d$ spin-up levels and one electron to the $3d$ spin-down orbital. A nonzero spin then is created due to the imbalance in the $3d$ occupations. Since the electron has a magnetic moment of 1 bohr magneton, μ_B, the magnetic moment of the Fe atom is $4\mu_B$. Therefore, one can see the potential of these systems as building blocks for novel information storage materials, where transition metal clusters retain high magnetic moments at reduced sizes.

Since the π-electron surface can influence the magnetic properties of transition metals, the choice of the organic molecules as substrates for these clusters becomes critical. Coronene ($C_{24}H_{12}$) is a polycyclic aromatic hydrocarbon (PAH). PAHs exist in many environments such as soot produced from hydrocarbon combustion. They are also believed to be present in many regions of the interstellar medium. Coronene is considered to be an extended system of benzene and thus can bind multiple metal atoms or clusters effectively. Metal-PAH complexes can also be used as models for metal binding to graphite or large diameter carbon nanotubes. Pozniak and Dunbar[32] studied Mg^+, Al^+, Si^+, In^+, Pb^+, and Bi^+ as well as the transition metal cations Sc^+ and Mn^+ coordinated with one or more coronene molecules. Positively charged $Sc_1(coronene)_{1,2}^+$ and $Mn_1(coronene)_{1,2}^+$ clusters were observed in their study. Duncan and co-workers generated $Cr_m(coronene)_n^+$ ($m=1-5$, $n=1-3$) (Ref. 33) and $Ag_m(coronene)_n^+$ ($m=1-3$, $n=1-4$) (Ref. 34) clusters. They proposed that the $Cr_m(coronene)_n^+$ clusters were multiple-decker sandwich structures. Duncan *et al.*[35] reported anion photoelectron spectroscopic studies of $V_m(coronene)_n^-$ and $Ti_m(coronene)_n^-$ ($m=1-5$, $n=1-3$) systems and provided interesting information about the geometries and electronic structures of those clusters, even though direct structural information was difficult to obtain. Later, our group reported a joint experimental and theoretical study of $Co_{1,2}(coronene)_1^-$ clusters,[36] in which the synergy between theory and experiment provided information about the geometries, electronic

a)Authors to whom correspondence should be addressed.
b)Electronic mail: kbowen@jhu.edu.
c)Electronic mail: akkandalam@vcu.edu.

structures, and magnetic properties of these cluster anions and their neutral counterparts. For $Co_{1,2}(coronene)_1^-$ and $Co_2(coronene)_1$ neutral, cobalt atoms prefer to minimize the number of Co-coronene bond interactions; i.e., the Co atom and its dimer prefer to occupy η^2-bridge bonding sites. For the $Co_1(coronene)_1$ neutral, there is a competition between the η^2- and η^6-ring binding sites.

Iron is an important element in part because it sits astride the first row of the transition metal atoms, and bulk iron has unique ferromagnetic properties. It is also known that while iron is among the most abundant elements in the universe,[37] its cosmic abundance in the interstellar medium is less than what would be expected.[38–40] Serra *et al.*[41] proposed that the reason for this depletion is the frequent collisions between iron and PAHs, leading to the formation of stable iron-PAH complexes. Some studies have been done for the Fe-coronene systems. Buchanan *et al.*[42] produced positively charged $Fe_m(coronene)_n^+$ ($m=1-3$, $n=1-5$) clusters by laser vaporization and studied them by photodissociation. They reported that iron binds to coronene as separated atoms and can form stable sandwich structures. Theoretical work done by Senapati *et al.*[43] disagreed with that conclusion, finding that Fe_2 dimers form strong bonds with coronene. Their calculation also showed that for neutral and cationic $Fe_1(coronene)_1$ clusters, the Fe atom is π-bonded to the coronene molecule and lies on top of the outer ring (η^6). Simon and Joblin[44] and Wang *et al.*[45] also did calculations on the $Fe_1(coronene)_1$ and related clusters. Here we study the negatively charged and neutral $Fe_m(coronene)_n$ ($m=1,2$, $n=1,2$) complexes by utilizing negative ion photoelectron spectroscopy and theoretical calculations. The combination of the two provides information on their geometrical and electronic structures and on their magnetic properties.

METHODS

A. Experiment

$Fe_m(coronene)_n^-$ ($m=1,2$, $n=1,2$) cluster anions were generated by laser vaporizing [Nd:YAG (yttrium aluminum garnet) laser, at 532 nm] a rotating, translating coronene coated iron rod. Helium from a pulsed valve induced clustering and cooled them. While we focused on the mixed metal-organic clusters that were produced by this source, signals of $coronene_n^-$ clusters were actually stronger in the mass spectrum. The $Fe_m(coronene)_n^-$ cluster anions were extracted into a linear time-of-flight mass spectrometer (mass resolution of ~600), mass selected, and photodetached with the third harmonic frequency (355 nm, 3.49 eV) of another Nd:YAG laser. The resulting photodetached electrons were then energy analyzed with a magnetic bottle electron energy analyzer having a resolution of ~50 meV at EKE=1 eV. The photodetachment process is governed by the energy-conserving relationship, $h\nu$=EBE+EKE—where $h\nu$ is the photon energy, EBE is the electron binding energy, and EKE is the electron kinetic energy—and by the selection rule that the multiplicity of the anion must change by ±1 as a result of photodetachment. Our anion photoelectron spectrometer has been described in detail previously.[46]

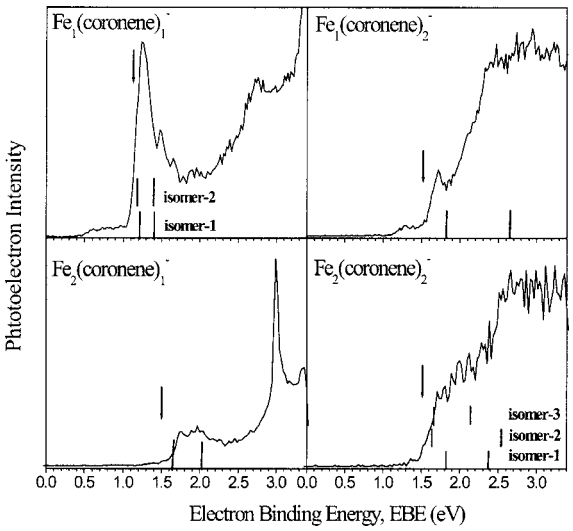

FIG. 1. The photoelectron spectra of $Fe_m(coronene)_n^-$ ($m=1,2$, $n=1,2$) complexes. The arrows indicate the calculated EA_a values, while the sticks represent the calculated photodetachment transition energies.

B. Computational

The ground state configurations and the ground spin states of neutral and negatively charged $Fe_m(coronene)_n$ complexes were obtained by density functional theory based electronic structure calculations. The gradient corrected Becke's exchange[47] functional, combined with the Perdew–Wang correlation[48] functional (referred to as BPW91), was used in these calculations. A relativistic effective core potential with a 16 electron valance basis set (Lan12*dz*) was adopted for the Fe atom, while a triple-ζ basis set (6-311G**) was used for the carbon and hydrogen atoms of the coronene molecule. All of the calculations were carried out using the GAUSSIAN 03 software package.[49] Several structural configurations of neutral and anionic $Fe_m(coronene)_n$ ($m,n=1,2$) complexes were optimized without any symmetry constraints for the various possible spin states. In the geometry optimization procedure, the convergence criterion for energy was set to 10^{-9} hartree, while the gradient was converged to 10^{-4} hartree/Å. The reliability and accuracy of the functional form and the basis sets used in this study in predicting the ground state geometries and the corresponding energetics have been established in our previous studies on $Co_m(coronene)_n$ (Ref. 36) and $V_n(benzene)_{n+1}$ complexes.[15]

In order to confirm the accuracy of the predicted ground state structures and their corresponding spin states, the adiabatic electron affinities (EA_a), vertical detachment energies (VDE), and other photodetachment transitions obtained from the theoretical calculations were compared with the corresponding measured values. The adiabatic EA is defined as the energy difference between the anion and the neutral systems when both are in their ground state geometries. The VDE is the energy between the ground state anion and its corresponding neutral at the geometry of the anion.

RESULTS AND DISCUSSION

The measured photoelectron spectra of $Fe_m(coronene)_n^-$ ($m=1,2$, $n=1,2$) are presented in Fig. 1. The downward

TABLE I. The calculated and experimental EA_a values and photodetachment transitions for $Fe_m(coronene)_n$ $(m=1,2;\ n=1,2)$. The first transition corresponds to the VDE value.

	EA_a (eV)		Photodetachment transitions (eV)		
	Theory	Experiment		Theory	Experiment
$Fe_1(coronene)_1$	1.02	1.06	Isomer-1	1.21	1.22
				1.40	1.50
			Isomer-2	1.19	
				1.40	
$Fe_2(coronene)_1$	1.48	1.59		1.64	1.73
				2.01	1.98
$Fe_1(coronene)_2$	1.51	1.50		1.82	1.71
				2.65	~2.5
$Fe_2(coronene)_2$	1.53	1.48	Isomer-1	1.81	
				2.37	···
			Isomer-2	1.62	
				2.54	
			Isomer-3	1.63	
				2.15	

pointing arrows on the spectra mark the EBE values that correspond to the calculated EA_a values, while the stick spectra indicate the EBE values of calculated photodetachment transition energies. The onset of the photoelectron spectrum reflects the EA_a value of the neutral species except when there is a poor Franck–Condon overlap between the lowest vibrational levels of the anion and its corresponding neutral or when there are significant vibrational hot bands present. The EBE values of peak maxima reflect a maximal Franck–Condon overlap for those particular photodetachment transitions. A comparison between our calculated and experimental values is presented in Table I. The calculated most stable structures of the $Fe_m(coronene)_n$ $(m=1,2,\ n=1,2)$ cluster anions and neutrals are shown in Figs. 2–8.

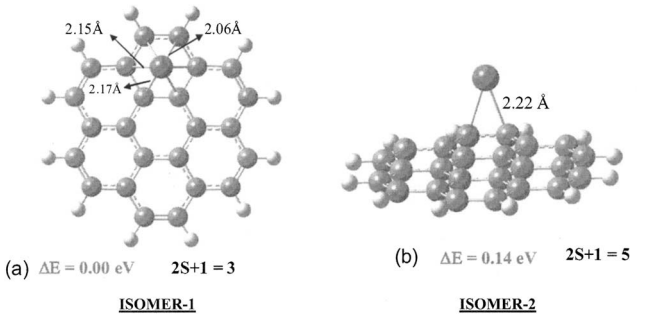

FIG. 3. The ground state isomer and the next higher energy isomer of the neutral $Fe_1(coronene)_1$ complex.

The calculated spin multiplicity $(2S+1)$ of each structure, as well as the photodetachment transitions resulting from a multiplicity change of ± 1, is also shown in these figures. The spin magnetic moment, in units of bohr magnetons (μ_B), is the spin multiplicity minus one $[(2S+1)-1=2S]$. Since orbital magnetic moment contributions are usually small in solids and we thus speculate in clusters, calculated spin magnetic moments are approximates to the total magnetic moments of clusters. The calculated per-atom magnetic moment for each cluster is listed in Table II, along with previous magnetic moment results for the iron atom, bulk iron, and other Fe-organic systems for comparison.

A. $Fe_1(coronene)_1^-$ and $Fe_1(coronene)_1$

The photoelectron spectrum of $Fe_1(coronene)_1^-$ (see Fig. 1) is dominated by a relatively strong sharp peak centered at EBE=1.22 eV with two (or more) nearby vibronic peaks centered at EBEs of 1.50 and 1.67 eV. At higher EBEs, another major band is centered at around 2.75 eV. The sharp portion of the onset in this spectrum occurs at 1.06 eV, and this value is interpreted to be the EA_a of the $Fe_1(coronene)_1$ neutral. The spectral profile of this spectrum is very similar

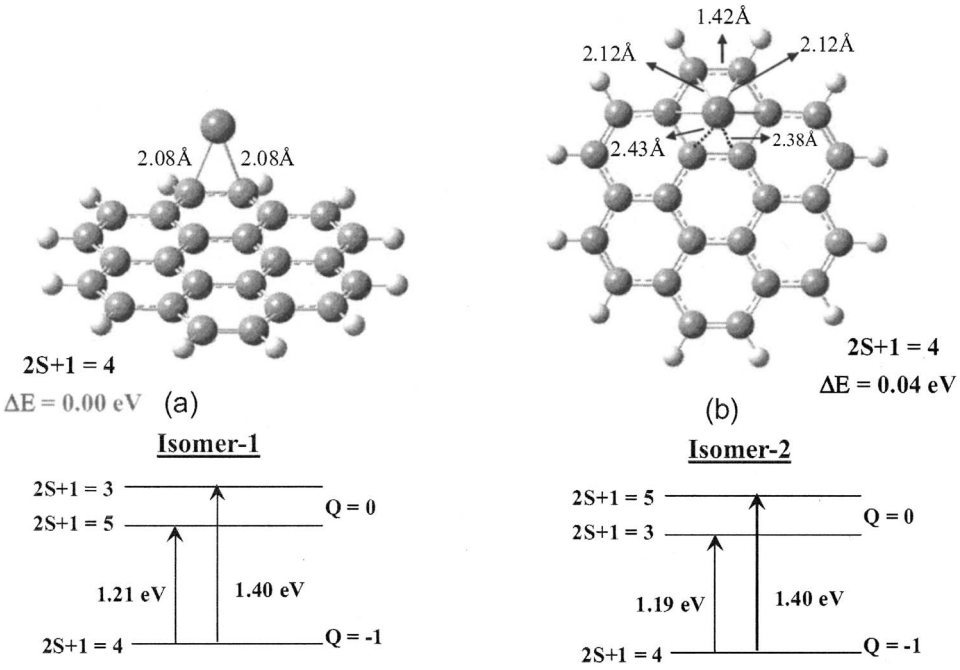

FIG. 2. The ground state isomer and the next higher energy isomer of the negatively charged $Fe_1(coronene)_1^-$ complex. The calculated photodetachment transition energies for each of these isomers are also shown.

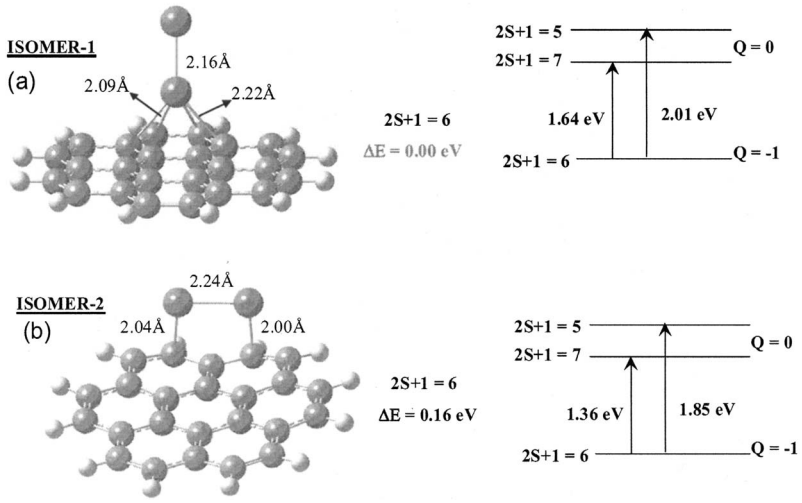

FIG. 4. The ground state isomer and the next higher energy isomer of the negatively charged $Fe_2(coronene)_1^-$ complex. The calculated photodetachment transition energies for each of these isomers are also shown.

to that of $Co_1(coronene)_1^-$ except for a small shift in the positions of the peaks. This implies similar geometrical and electronic structures for the two systems.

The calculated lowest energy and the next higher energy isomer of the negatively charged $Fe(coronene)^-$ complex are shown in Fig. 2. In the lowest energy structure, the Fe atom binds to a η^2-type C–C bridge site of the peripheral ring of the coronene molecule [Fig. 2(a), isomer-1]. There is another energetically degenerate isomer (0.04 eV higher in energy) in which the Fe atom prefers to occupy the on-top site (η^6) above the center of the peripheral ring of the coronene [Fig. 2(b), isomer-2]. Since the energy difference falls within the computational uncertainty (~0.20 eV) of the present theoretical method, the ground state geometry of $Fe_1(coronene)_1^-$ could be either of these isomers. A similar pattern was observed in our earlier study on the $Co(coronene)^-$ complex,[36] where the energy difference between the structures containing η^2- and η^6-coordinated Co was found to be 0.25 eV, with the η^2-binding site again being more preferable. By comparing the calculated photodetachment transition energies with peaks in the experimental spectrum, one should, in principle, be able to distinguish between the two isomers. For the lowest energy (η^2-coordinated) isomer, the calculated transitions are 1.21 and 1.40 eV, corresponding to the transitions from the anion quartet to the neutral quintet and triplet states, respectively. As for the η^6 -coordinated isomer, the calculated transitions are 1.19 eV (quartet to triplet) and 1.40 eV (quartet to quintet). Thus, the calculated values of both the isomers are in good agreement with the measured transitions of 1.22 and 1.50 eV, either making it difficult to distinguish between them or possibly indicating the existence of both isomers in the beam. Furthermore, even though both isomers have similar transition energies, there are electronic structural differences. These are reflected in the nature of frontier molecular orbitals (MOs), which are shown in Fig. 9, and they are evident in the detachment of the first electron from them. In the case of the η^2-coordinated isomer [Figure 9(a)], the lowest energy transition corresponds to electron

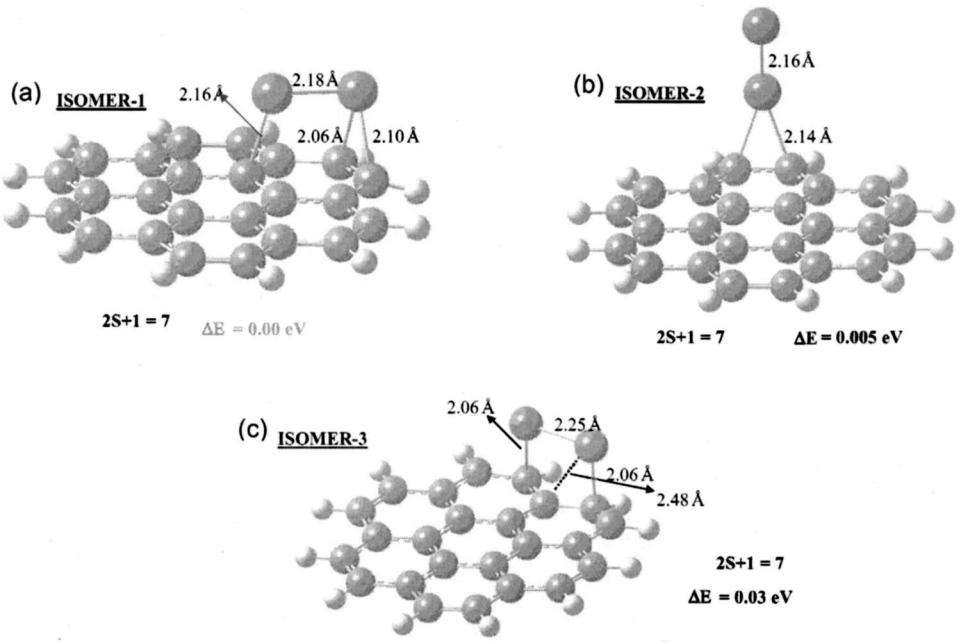

FIG. 5. The ground state isomer and the next higher energy isomers of the neutral $Fe_2(coronene)_1$ complex. The spin multiplicities and the relative energies (in eV) are also shown.

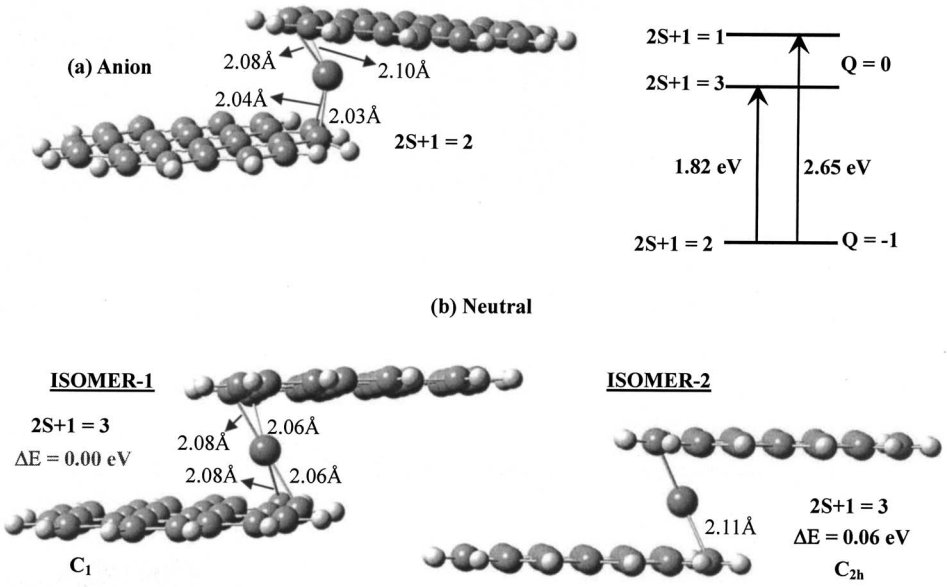

FIG. 6. (a) The ground state isomer of the negatively charged $Fe_1(coronene)_2^-$ complex. (b) The ground state and the next higher energy isomer of the neutral $Fe_1(coronene)_2$ complex. The calculated photodetachment transition energies for the ground state anion are also shown.

detachment from a nonbonding β-MO resulting in a neutral quintet state, whereas in the η^6-coordinated isomer [Fig. 9(b)] the first electron detachment is from a d_z^2 antibonding α-MO, thus resulting in a neutral triplet state. In addition, it was also seen that the frontier orbitals of the η^2-coordinated isomer are dominated mostly by nonbonding orbitals mainly located on the metal atom, whereas in the case of the η^6 -coordinated isomer, the frontier orbitals are dominated by either antibonding or bonding orbitals. For example, the α-(HOMO-1) (HOMO stands for highest occupied molecular orbital) and β-HOMO are both bonding orbitals with bonding characteristics between d_z^2 of Fe and π orbitals of coronene in α-(HOMO-1) and between d_{yz} of Fe and π orbitals of coronene in β-HOMO.

For the neutral $Fe_1(coronene)_1$ complex, the iron atom prefers to bind to the η^6 -site of the peripheral ring of the coronene [see Fig. 3(a)]. However, the structure with η^2 -binding of Fe atom is less stable by only 0.14 eV [see Fig. 3(b)]. Thus, the competition between the η^2- and η^6-binding sites is observed again, but this time for the neutral system. The calculated EA_a value of 1.02 eV is in excellent agreement with the measured value of 1.06 eV. We can also compare the EAs of molecular coronene (0.47 and 0.54 eV) (Refs. 50 and 51) and the iron atom (0.15 eV) (Ref. 53) with the $Fe_1(coronene)_1$ complex (1.06 eV). While the EAs of both moieties are positive, our calculation showed that the excess electron resides mostly on the Fe moiety. Thus coronene is polarizible enough to provide 0.91 eV in complexation energy, i.e., 0.15+0.91 eV=1.06 eV. This energy is much higher than that for the $Co_1(coronene)_1^-$ complex, i.e., 0.49 eV.[36] Also, since the photoelectron spectrum of the $Fe_1(coronene)_1^-$ complex does not show the characteristic profiles of either the atomic iron anion's or the coronene anion's photoelectron spectrum, $Fe_1(coronene)_1^-$ is seen not to be an anion-neutral molecule complex. The interaction between the two moieties is apparently quite complex.

Now we turn to the magnetic properties of the neutral

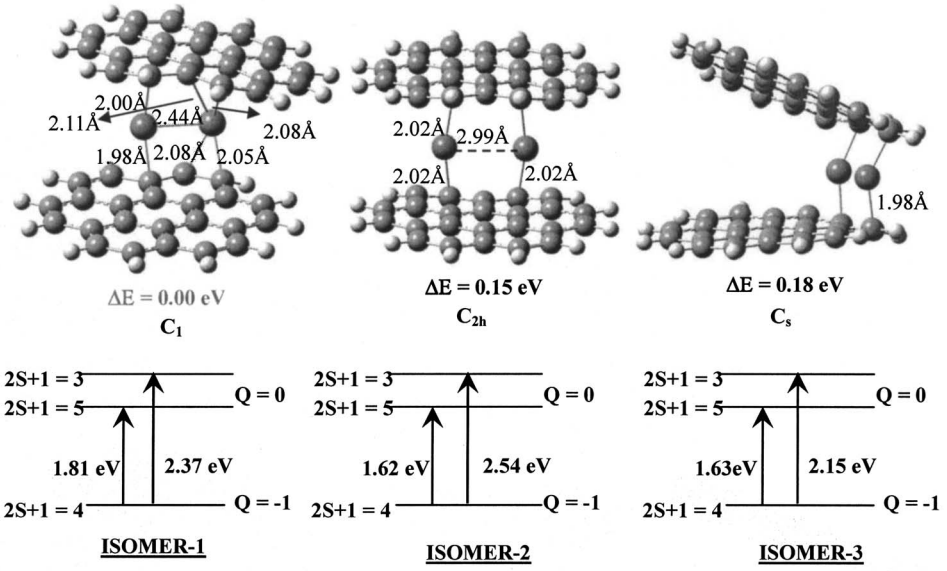

FIG. 7. The three most stable structural configurations of the negatively charged $Fe_2(coronene)_2$ complex. The calculated photodetachment transition energies for each of these isomers are also shown.

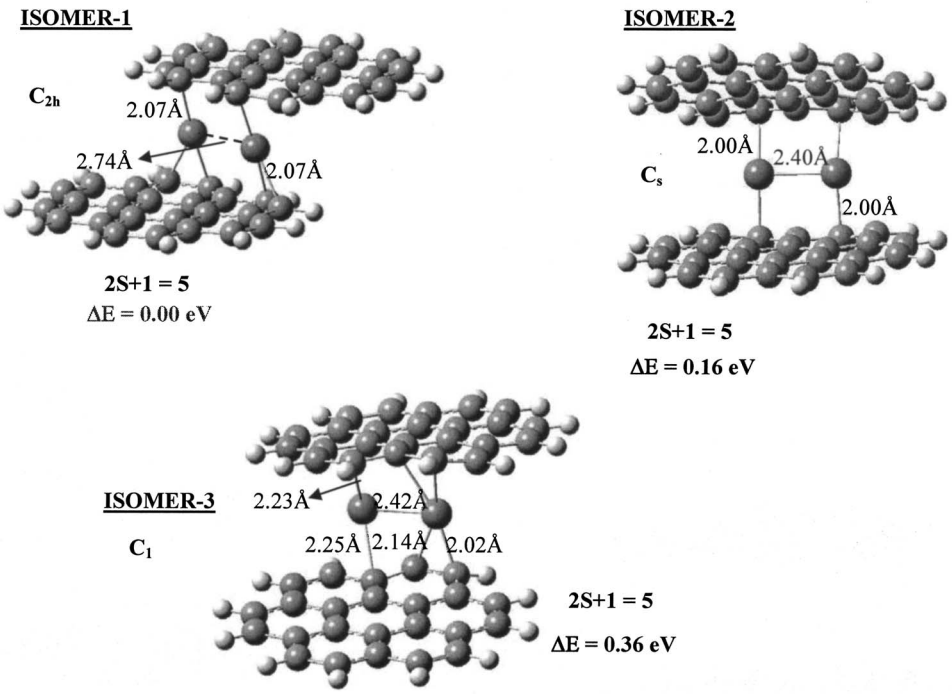

FIG. 8. The three most stable isomers of the neutral Fe_2(coronene)$_2$ complex. Isomer-1 and isomer-3 are staggered sandwiches, while isomer-2 is a normal (partially eclipsed) sandwich. The preferred spin multiplicity and the symmetry of each of the isomers along with the relative energies (in eV) are also shown.

Fe(coronene) system. The ground state spin multiplicities of the two energetically identical isomers differ: while the triplet spin state ($2S+1=3$) is the preferred spin state of the lowest energy isomer, the isomer with η^2-binding of Fe atom prefers a quintet spin state ($2S+1=5$). Since these two spin states are almost energetically degenerate (within the uncertainty of theory), there is the possibility of the metal atom retaining its high atomic spin of 4 when an Fe atom interacts with a coronene molecule. If we focus on the high spin state, i.e., quintet, we get a magnetic moment of $(2S+1)-1=5-1=4\mu_B$. It is interesting to compare this magnetic moment result with previous results for atomic Fe, bulk Fe, and Fe interacting with other organic molecules. It is known that the magnetic moment of free Fe is $4\mu_B$,[53] and that of the bulk material is much smaller [$2.2\mu_B$ (Refs. 54–56)]. As mentioned above, the magnetic moment of transition metal clusters increases dramatically with reduced size (30–60% in several cases), and it further changes upon the interaction of transition metals with an organic surface. Previous studies on Fe_1(benzene)$_1$ and Fe_1(benzene)$_2$ showed[13,14] that the magnetic moments of these systems are both $2\mu_B$ (see Table II).

TABLE II. The per-atom magnetic moments for Fe bulk, Fe free atom, Fe dimer, and Fe-organic systems.

System	Per-atom magnetic moment (μ_B)
Fe bulk	2.2 (Refs. 51–53)
Fe free atom	4 (Ref. 50)
Fe(coronene)	4
Fe(coronene)$_2$	2
Fe(benzene)$_1$	2 (Refs. 13 and 14)
Fe(benzene)$_2$	2 (Ref. 13)
Fe_2	3 (Ref. 63)
Fe_2(coronene)	3
Fe_2(coronene)$_2$	2

Thus while interacting with atomic Fe, neither of the single or double benzene complexes retained the high magnetic moment of atomic Fe; rather, the value was lowered below the bulk value. Coronene, on the contrary, provides the possibility to retain the high magnetic moment present in the free Fe atom. Nevertheless, in Fe(coronene) there is only one iron atom and one coronene. One must study the magnetic properties of multiple Fe atoms deposited on multiple coronene molecules to begin to draw conclusions. It is worth noting here that a similar result was not found for the Co_1(coronene)$_1$ system.[36] The magnetic moment of Co_1(coronene)$_1$ reduced to $1\mu_B$ compared to a free cobalt atom of $3\mu_B$ (the bulk value for cobalt is $1.7\mu_B$). This suggests that for different transition metals, different organic surfaces are required to retain their high magnetic moments at reduced sizes.

Our calculated lowest energy structure and the spin multiplicity of the neutral Fe_1(coronene)$_1$ complex agree with previous theoretical work by Senapati *et al.*[43] However, in that study the authors did not consider the η^2-binding of Fe to coronene molecule. In an earlier experimental and theoretical study[45] of the vibrational spectroscopy of neutral Fe(PAH) complexes, the Fe atom preferred the η^6-site, and the ground state multiplicity of the Fe_1(coronene)$_1$ was reported as a triplet. However, this study also did not consider the η^2 versus η^6 competition in stabilizing the Fe_1(coronene)$_1$ complex. Interestingly, in the calculation of Simon and Joblin[44] on the same system, the authors found that the Fe atom prefers the η^2-binding site with a spin multiplicity of 5 (quintet).

B. Fe_2(coronene)$_1^-$ and Fe_2(coronene)$_1$

The photoelectron spectrum of Fe_2(coronene)$_1^-$ (see Fig. 1) has an onset at ~1.59 eV, which we interpret to be the EA_a of the corresponding neutral. The lowest discernible

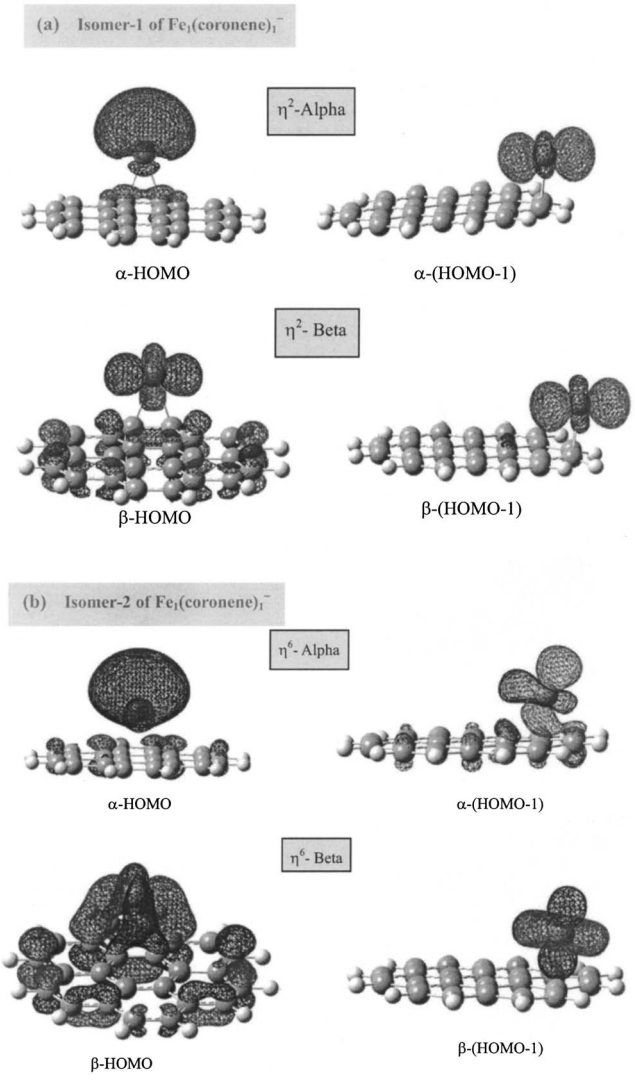

FIG. 9. Frontier orbitals of (a) isomer-1 and (b) isomer-2 of the $Fe_1(coronene)_1^-$ complex. The MO surfaces are obtained at an isovalue of ±0.03 using GAUSSVIEW.

peak appears at EBE=1.73 eV, followed by a set of peaks having similar intensities and centered around 1.98 eV. The strongest and narrowest peak in the spectrum occurs at EBE=2.97 eV. There appears to be still another peak at 3.33 eV. Thus, the photodetachment transition energies evident in this spectrum occur at EBE=1.73, 1.98, 2.97, and 3.33 eV. Theoretical calculations predict two structural isomers for $Fe_2(coronene)_1^-$, separated by an energy difference of 0.16 eV (see Fig. 4). In both isomers, the iron atoms dimerize and bind to the coronene molecule. For the lowest energy isomer [see Fig. 4(a)], the bond axis of the Fe_2 dimer is found to be almost perpendicular to the coronene molecule, with only one Fe atom directly interacting with coronene via η^6-type bonding. The Fe–Fe bond length in this isomer is calculated to be 2.16 Å compared to the free Fe_2 dimer bond length of 2.03 Å. A similar structure was observed in our earlier study[36] on $Co_2(coronene)_1^-$ complex, except that there the cobalt dimer was bound perpendicularly to the bridge site (η^2) of the outer ring of coronene. Interestingly, the η^2-binding site was not a minimum on the

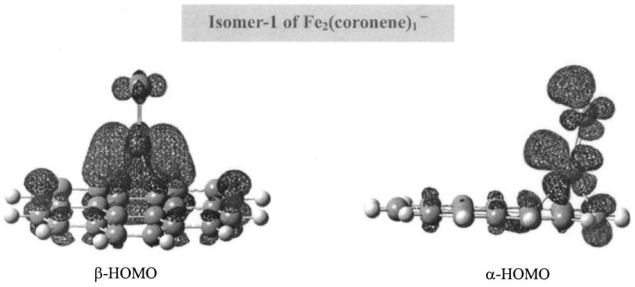

FIG. 10. Frontier orbitals of isomer-1 of the $Fe_2(coronene)_1^-$ complex. The MO surfaces are obtained at an isovalue of ±0.03 using GAUSSVIEW.

$Fe_2(coronene)_1^-$ potential energy surface. In the next higher energy isomer of $Fe_2(coronene)_1^-$ [Fig. 4(b)], both the iron atoms bind to the edge carbons of the adjacent peripheral rings of coronene. This isomer is similar to the corresponding higher energy isomer of the $Co_2(coronene)_1^-$ complex. The Fe–Fe bond length in this higher energy isomer is elongated (2.24 Å) compared to the 2.16 Å Fe–Fe bond length in the lowest energy isomer. The spin multiplicity of both $Fe_2(coronene)_1^-$ isomers is predicted to be a sextet ($2S+1=6$). The calculated transitions from the anions' sextet state to neutrals' septet and quintet for both structures are given in Fig. 4. The calculated transitions are 1.64 eV (sextet to septet) and 2.01 eV (sextet to quintet) for the most stable isomer, and 1.36 eV (sextet to septet) and 1.85 eV (sextet to quintet) for the higher energy isomer. By comparing these with the experimentally measured transition energies for the first two transitions (1.73 and 1.98 eV), we conclude (despite the small energy difference between the two isomers) that only the most stable isomer [Fig. 4(a)] was observed experimentally.

An analysis of the electronic structure of the lowest energy $Fe_2(coronene)_1^-$ sextet complex revealed that the calculated VDE of 1.64 eV is the result of an electron detachment from a β-MO, dominated by bonding between the d_{xy} orbital of the proximal Fe atom and the p orbital of carbon atoms with a minor contribution from the d_{xy} orbital of the distal Fe atom (see Fig. 10). The first transition to the neutral triplet state (2.01 eV) corresponds to the electron detachment from the antibonding orbital located on the metal atoms. This is in contrast with the electronic structure of the $Co_2(coronene)_1^-$ complex,[36] where the two lowest electron detachment energies are due to the electron detachment from the d_z^2 antibonding orbital between the Co atoms. In $Co_2(coronene)_1^-$ the frontier orbitals are dominated by either antibonding or nonbonding orbitals located on the metal atoms, while in $Fe_2(coronene)_1^-$ the nature of frontier orbitals are more complex with contributions not only from the distal Fe atom but also from the proximal Fe and coronene molecule. Therefore, we conclude that even though the structural differences between the $Fe_2(coronene)_1^-$ and previously reported $Co_2(coronene)_1^-$ complexes are minor, major differences in their electronic structures explain why the photoelectron spectra of $Co_2(coronene)_1^-$ and $Fe_2(coronene)_1^-$ are so dissimilar. These differences may also explain why we see similarities between the photoelectron spectra of $Co_2(coronene)_1^-$ and those of Co^- but dissimilarities be-

tween the spectra of $Fe_2(coronene)_1^-$ and Fe^-. The spectrum of $Co_2(coronene)_1^-$ showed the spectral characteristics of Co^- rather than of Co_2^- because the extra charge is mostly localized on the dangling Co atom.[36] However for $Fe_2(coronene)_1^-$, the electronic structure is very different from its Co counterpart due to a more complicated interaction, and this results in the photoelectron spectrum of $Fe_2(coronene)_1^-$ showing no significant similarity to either Fe^- or Fe_2^-.

For the $Fe_2(coronene)_1$ neutral cluster, the calculations predict three structural isomers that are very close in energy. The three isomers are shown in Fig. 5. The calculated EA_a is 1.48 eV, which is in agreement with our measured value of 1.59 eV. In isomer-1 [Fig. 5(a)], the Fe_2 dimer binds to the edges of the peripheral ring of the coronene (η^2-binding), with its bond axis parallel to the coronene molecule. Isomer-2 is similar to the ground state structure of the $Fe_2(coronene)_1^-$ anion complex, which has only one Fe atom directly interacting with the coronene and the Fe_2 dimer bond axis perpendicular to the coronene surface [Fig. 5(b)]. However, in the case of the neutral complex, the interacting (proximal) Fe atom occupies the η^2-bridge site of the peripheral ring of coronene as opposed to the η^6-binding found in the anion. The isomers-1 and -2 are found to be energetically degenerate with an energy difference of only 0.005 eV, with Fe–Fe bond lengths of 2.18 and 2.16 Å, respectively. The next higher energy structure, isomer-3, is 0.03 eV higher in energy, and it has two iron atoms binding to the C–C bonds of two adjacent outer rings of the coronene [Fig. 5(c)]. The distance between Fe atoms in this isomer is 2.25 Å, considerably elongated from the Fe_2 dimer bond length of 2.03 Å. Note that the isomer-3 is similar to the higher energy isomer [Fig. 4(b)] seen in the anion. Senapati *et al.* in an earlier study[43] also found that Fe atoms dimerize on the coronene molecule. However, the relative energies of the lowest energy isomers obtained in our work differ from their earlier findings. For example, in the work of Senapati *et al.*,[43] the lowest energy structure corresponds to the Fe atoms binding to the η^6-sites of adjacent outer rings of coronene, and the next higher energy isomer (ΔE=0.16 eV) corresponds to Fe_2 dimer binding to the bridge (η^2) sites of the peripheral ring. Our lowest energy isomer is similar to their higher energy isomer. Interestingly, the ground state geometry reported in that work, according to our calculations, does not correspond to a local minimum. When Fe atoms are placed above the center of adjacent peripheral rings, the Fe atoms move away from the center of the ring onto the edge of the peripheral rings during geometry optimization. A similar situation was observed in our earlier reported work on the $Co_2(coronene)$ complex. In addition, we found another stable structure, isomer-2, in this study, which was not seen in the work of Senapati *et al.*[43] The notable structural feature appearing in all of the three lowest energy isomers is that the iron prefers to form a dimmer while interacting with the coronene molecule, which is in good agreement with the previous work[43] of Senapati *et al.* The structural configurations where the Fe atoms bind separately to the coronene are found to be very high in energy. Buchanan *et al.*[42] previously interpreted their photodissociation experiments on $Fe_2^+(coronene)_1$, showing that Fe atoms bind to coronene separately. Our results, however, show that in the case of neutral and anion $Fe_2(coronene)$ complexes, the Fe atoms always form a dimer and interact with the coronene molecule.

The calculated ground state spin multiplicity of all the three isomers is found to be a septet ($2S+1=7$), which indicates a magnetic moment of $(2S+1)-1=7-1=6\mu_B$. Since there are two Fe atoms in the cluster, the magnetic moment for each Fe atom is $6\mu_B/2=3\mu_B$. Compare this value to that of Fe_2, where there are $3\mu_B$ per atom. Again, the Fe_2 dimer moiety within the $Fe_2(coronene)_1$ complex retains its high magnetic moment, just as Fe did in the $Fe_1(coronene)_1$ complex.

C. $Fe_1(coronene)_2^-$ and $Fe_1(coronene)_2$

In the photoelectron spectrum of $Fe_1(coronene)_2^-$, we observed a ledgelike spectral feature at EBE ~1.3 eV followed by a peak at 1.71 eV. A more intense and broad band (or a mixture of several bands) covers the high EBE area from ~1.85 eV up to the edge of our energy window. The signal around 1.3 eV is believed to be a hot band because the intensity there varied with source conditions. Hence, the onset of the spectrum and our selection for the EA_a value is 1.50 eV. Our calculations found the most stable structure of $Fe_1(coronene)_2^-$ to be a staggered sandwich, with the Fe atom sandwiched between the two coronene molecules [Fig. 6(a)]. The Fe atom binds to η^2-bridge sites on the terminal rings of both coronene molecules. The two coronene planes are rotated away from one another, leaving one terminal ring on top of another but not exactly overlapping. Note that the coronene planes are not parallel to each other either. The spin multiplicity of this isomer is doublet ($2S+1=2$). The calculated energies for the first two vertical transitions are 1.82 and 2.65 eV, corresponding to the transitions from the anion doublet state of the anion to the neutral triplet and singlet states, respectively. The match with the experimental data is quite good.

For neutral $Fe_1(coronene)_2$, two competing isomers are found to be most stable with only a 0.06 eV difference in energy [Fig. 6(b)]. The two isomers have very similar geometries in terms of how the iron atom is staggered and sandwiched between two coronene molecules and how the iron sits on top of a terminal ring (η^6) of each coronene. The two terminal rings to which the iron binds overlap with one another. The second most stable isomer has two coronene molecules parallel to each other, although in the most stable isomer, one coronene is tilted relative to the other. The calculated EA_a is 1.51 eV, which is in excellent agreement with the measured value, 1.50 eV. The calculated spin multiplicities for the most stable $Fe_1(coronene)_2$ neutral isomers are both $2S+1=3$; thus the magnetic moment is $3-1=2\mu_B$. Although one coronene molecule can retain the high magnetic moment ($4\mu_B$) of the iron atom, when two coronene molecules interact with an iron atom, the magnetic moment appears to be reduced, becoming close to the bulk value of $2.2\mu_B$.

Even though the two coronene planes are not exactly parallel to each other in both the anionic and the most stable

neutral $Fe_1(coronene)_2$ complexes, the calculations find staggered sandwich structures; i.e., coronene molecules have only one outer ring overlapped and are linked by the metal atom only. Thus, together, our experimental and computational results provide evidence for the existence of sandwich structures for transition metal–coronene complexes. In an earlier work by Foster *et al.*,[33] the authors proposed a staggered sandwich structure as a possible structure for $Cr_1(coronene)_2^+$. The metal binding was thought to transfer charge to both rings, giving the coronene rings similar charge densities, which in turn caused the two coronene molecules to rotate away from one another and to form a staggered configuration. Our calculations likewise confirm this scenario for the $Fe_1(coronene)_2$ system. In view of our current results along with the previous work, it appears that sandwich structures in TM-coronene complexes are common for both their neutral and charged states. Furthermore, multiple-decker sandwich structures can be expected in these systems as well.

D. $Fe_2(coronene)_2^-$ and $Fe_2(coronene)_2$

The photoelectron spectrum of $Fe_2(coronene)_2^-$ lacks a significant structure, although at least two bands are discernible. One band starts at 1.48 eV and continues until ~2.4 eV. There, another band begins and covers the remaining EBE range out to the edge of our energy window. We take 1.48 eV to be the EA_a value. Three isomers are found theoretically for $Fe_2(coronene)_2^-$, and they are shown in Fig. 7. The quartet $(2S+1=4)$ spin state is found to be the ground spin multiplicity of the three isomers. The ground state structure, isomer-1, is a staggered sandwich, with the two coronene molecules connected by the iron dimer between them. The iron atoms bind to the η^2-bridge sites of the outer rings. There is little overlapping between the coronene molecules, and because of metal dimer binding, the coronene planes are not parallel. This structure has a C_1 symmetry. The calculated first two transitions for this isomer are 1.81 and 2.37 eV, corresponding to transitions from anion quartet to neutral quintet and neutral triplet states, respectively. The next higher energy isomer (isomer-2) is 0.15 eV above the ground state, and its structure is a similar staggered sandwich, with the coronene molecules linked by an iron dimer. This isomer has a higher symmetry (C_{2h}) because the iron atoms sit exactly in between the two exactly parallel coronene molecules. However, the Fe–Fe distance in this isomer has elongated to 2.99 Å. The calculated vertical transitions for isomer-2 are 1.62 eV (quartet to quintet) and 2.54 eV (quartet to triplet). The isomer-3, which is 0.18 eV less stable than the ground state, also adopts a sandwich structure, with the iron dimer binding to the η^2-bridge sites on the outer rings of coronene molecules. Differing from the more stable structures, the interaction between the iron dimer and the coronene molecules pulls the ends of both coronene molecules together, while allowing the opposite ends of coronene molecules to bend away from each other. The calculated transitions are 1.63 eV (quartet to quintet) and 2.15 eV (quartet to triplet). It is difficult to correlate one particular isomer with our photoelectron spectrum. The broad bands may indicate that the mixture of two or three isomers could contribute to the photoelectron signal.

For neutral $Fe_2(coronene)_2$, there are also three stable isomers that have been predicted by the calculations (see Fig. 8). The calculated EA_a of 1.53 eV matches the experimental value of 1.48 eV very well. Similar to the anion, these isomers all prefer sandwich structures, either a staggered sandwich or a regular sandwich, with the iron dimer connecting the coronene molecules. The most stable isomer adopts a C_{2h} staggered sandwich structure with a Fe–Fe bond length of 2.74 Å. The two terminal rings of both coronene molecules are linked by the iron dimer and overlapped with each other. The second and third most stable structures have C_s and C_1 symmetries and are 0.16 and 0.36 eV less stable, respectively. It is worth noting that the most stable neutral isomer has a C_{2h} symmetry, while the most stable isomer in anion has a C_1 symmetry. Thus, a charge-induced symmetry breaking in the $Fe_2(coronene)_2$ complex is observed here.

Both the neutral and anionic species of $Fe_2(coronene)_2$ appear to prefer sandwich structures with both iron atoms located between the coronene molecules. Hence, the formation of a multiple layer type, $|\cdot|\cdot$, of sandwich complex is not preferred. These results further support our conclusion that Fe atoms, when deposited on coronene, would prefer to form a dimer rather than bind to coronene as individual atoms. Furthermore, the metal atoms tend to sit on the edge of both coronene molecules, and since there are several binding sites available on the coronene, it is reasonable to believe that larger metal clusters can link coronene molecules to form a sandwich structure.

The coupling between the Fe atoms in neutral $Fe_2(coronene)_2$ is again found to be ferromagnetic in nature. The calculated ground state spin multiplicity of neutral $Fe_2(coronene)_2$ is a quintet $(2S+1=5)$, which makes the total magnetic moment of $Fe_2(coronene)_2$ $4\mu_B$; thus the moment for each iron atom is $2\mu_B$. Again, we compare this value with the magnetic moment of Fe_2, i.e., $3\mu_B$ per atom. It is clear that the two coronene molecules do not allow the magnetic moment of the iron dimer to be retained, instead reducing it toward the bulk value $(2.2\mu_B)$. This is consistent with what was seen for $Fe_1(coronene)_2^-$.

E. Summary and outlook

Although metal binding to the center ring of coronene generates a structure with a pleasing symmetry, previous theoretical work[57,58] indicates that the outer rings of coronene are the favored locations for metal binding, and indeed complexes with such structures (e.g., cyclopentadienyl-iron-coronene) have been synthesized.[59–61] Among the structures we reported here, none has the metal atom or dimer binding to the center ring of the coronene, including the sandwich structures. The iron atom binds to the bridge site of coronene in $Fe_1(coronene)_1$, which is different from Ti_1-, V_1-, and $Co_1(coronene)_1$ systems.[36,62] $Fe_2(coronene)_1$ is similar to $Co_2(coronene)_1$ in that only one metal atom interacts with coronene, although Fe has a more complex interaction with coronene than does Co. Since there are many available bind-

ing sites and the metals prefer to bind on the same side of coronene, a significant number of metal atoms may be required to saturate the coronene ring. Although Buchanan *et al.*[42] produced and studied the cationic Fe-coronene cluster and suggested that three Fe atoms would saturate the coronene molecule, the situation for the corresponding anionic clusters may not necessarily be the same, and further experiments are needed in order to answer this question. The synergy of experiment and theory has provided evidence for the existence of sandwich structures for TM-coronene systems: more specifically, both $Fe_1(coronene)_2$ and $Fe_2(coronene)_2$ form staggered sandwich structures.

Another interesting observation for $Fe_2(coronene)_{1,2}$ systems is that none of the structures have the metal atoms being separated by coronene. This is contrary to previous work[42] on cation systems, $Fe_x(coronene)_2^+$. Certainly, we still expect the multiple-decker sandwich structure with the metal atoms being separated by coronene, but here we saw that the iron atoms tend to form a dimer with that cluster binding to coronene(s) as a complete moiety. Although the bond length between the metal atoms varies, they should not be considered as completely dispersed atoms. Thus, the structure proposed before,[33] with metal atoms binding to the alternate rings of coronene, may not always be the case.

One of the main targets of this study is aimed at answering a critical question that directly affects nanotechnology, especially with regard to information storage and processing. How will the interaction between the transition metal atom or clusters and their host substrate affect the magnetic moment of the atom or clusters? Our results could guide further gas phase and condensed phase synthesis for Fe-coronene or similar TM-coronene systems. The summarized previous and current results are shown in Table II. Note that the interaction with a single coronene molecule, as in Fe(coronene) and Fe_2(coronene), permits the complex to retain the magnetic moment of the Fe atom and the Fe dimer, respectively. The addition of another coronene molecule, however, causes the magnetic moment of the complex to fall below that of the bulk. Therefore, a single molecule coronene surface may be a good substrate for iron clusters, while double coronene surfaces do not play the same role. We cannot conclude that this is a general rule, however, because our previous study on $Co_{1,2}(coronene)_1$ showed that the single coronene molecule does not retain the magnetic moments of Co and Co dimer,[36] and our current study only deals with the systems having up to two iron atoms. Therefore, different types and sizes of the metal atoms or clusters may require specific surfaces to retain their magnetic moments. Further spectroscopic experimental and theoretical studies are needed.

ACKNOWLEDGMENTS

K.H.B. thanks the Division of Materials Science, Basic Energy Sciences, U.S. Department of Energy for support of this work under Grant No. DE-FG02-95ER45538. A.K.K. and P.J. acknowledge support from the U.S. Department of Energy under Grant No. DE-FG02-96ER45579.

[1] F. Meyer, F. A. Khan, and P. B. Armentrout, J. Acoust. Soc. Am. **117**, 9740 (1995).
[2] Y.-M. Chen and P. B. Armentrout, Chem. Phys. Lett. **210**, 123 (1993).
[3] F. Willey, C. S. Yeh, D. L. Robbins, and M. A. Duncan, J. Phys. Chem. **96**, 9106 (1992).
[4] D. van Heijnsbergen, G. von Helden, G. Meijer, P. Maitre, and M. A. Duncan, J. Am. Chem. Soc. **124**, 1562 (2002).
[5] P. Weis, P. R. Kemper, and M. T. Bowers, J. Phys. Chem. A **101**, 8207 (1997).
[6] C. Y. Lin, Q. Chen, H. Chen, and B. S. Freiser, J. Phys. Chem. A **101**, 6023 (1997).
[7] K. Hoshino, T. Kurikawa, H. Takeda, A. Nakajima, and K. Kaya, J. Phys. Chem. **99**, 3053 (1995).
[8] W.-J. Zheng, J. M. Nilles, O. C. Thomas, and K. H. Bowen, Chem. Phys. Lett. **401**, 266 (2005).
[9] W.-J. Zheng, J. M. Nilles, O. C. Thomas, and K. H. Bowen, J. Chem. Phys. **122**, 044306 (2005).
[10] T. Kurikawa, H. Takeda, M. Hirano, K. Judai, T. Arita, S. Nagao, A. Nakajima, and K. Kaya, Organometallics **18**, 1430 (1999).
[11] M. Gerhards, O. C. Thomas, J. M. Nilles, W.-J. Zheng, and K. H. Bowen, J. Chem. Phys. **116**, 10247 (2002).
[12] T. Kurikawa, H. Takeda, A. Nakajima, and K. Kaya, Z. Phys. D: At., Mol. Clusters **40**, 65 (1997).
[13] R. Pandey, B. K. Rao, P. Jena, and M. A. Blanco, J. Am. Chem. Soc. **123**, 3799 (2001).
[14] R. Pandey, B. K. Rao, P. Jena, and J. M. Newsam, Chem. Phys. Lett. **321**, 142 (2000).
[15] A. K. Kandalam, B. K. Rao, and P. Jena, J. Chem. Phys. **120**, 10414 (2004).
[16] B. K. Rao and P. Jena, J. Chem. Phys. **116**, 1343 (2002).
[17] B. K. Rao and P. Jena, J. Chem. Phys. **117**, 5234 (2002).
[18] W. A. de Heer, P. Milani, and A. Châtelain, Phys. Rev. Lett. **65**, 488 (1990).
[19] W. de Heer, P. Milani, and A. Châtelain, Z. Phys. D: At., Mol. Clusters **19**, 241 (1991).
[20] J. A. Becker and W. A. de Heer, Ber. Bunsenges. Phys. Chem. **96**, 1237 (1992).
[21] I. M. L. Billas, A. Châtelain, and W. A. de Heer, Science **265**, 1682 (1994).
[22] J. P. Bucher, D. C. Douglass, and L. A. Bloomfield, Phys. Rev. Lett. **66**, 3052 (1991).
[23] J. P. Bucher, D. C. Douglass, P. Xia, B. Haynes, and L. A. Bloomfield, Z. Phys. D: At., Mol. Clusters **19**, 251 (1991).
[24] D. C. Douglass, A. J. Cox, J. P. Bucher, and L. A. Bloomfield, Phys. Rev. B **47**, 12874 (1993).
[25] T. Hihara, S. Pokrant, and J. A. Becker, Chem. Phys. Lett. **294**, 357 (1998).
[26] M. B. Knickelbein, J. Chem. Phys. **115**, 1983 (2001).
[27] X. Xu, S. Yin, R. Moro, and W. de Heer, Phys. Rev. Lett. **95**, 237209 (2005).
[28] S. E. Apsel, J. W. Emmert, J. Deng, and L. A. Bloomfield, Phys. Rev. Lett. **76**, 1441 (1996).
[29] M. B. Knickelbein, J. Chem. Phys. **116**, 9703 (2002).
[30] M. B. Knickelbein, Chem. Phys. Lett. **353**, 221 (2002).
[31] M. B. Knickelbein, J. Chem. Phys. **125**, 044308 (2006).
[32] B. P. Pozniak and R. C. Dunbar, J. Am. Chem. Soc. **119**, 10439 (1997).
[33] N. R. Foster, G. A. Grieves, J. W. Buchanan, N. D. Flynn, and M. A. Duncan, J. Phys. Chem. A **104**, 11055 (2000).
[34] J. W. Buchanan, G. A. Grieves, N. D. Flynn, and M. A. Duncan, Int. J. Mass. Spectrom. **185–187**, 617 (1999).
[35] M. A. Duncan, A. M. Knight, Y. Negishi, S. Nagao, K. Judai, A. Nakajima, and K. Kaya, J. Phys. Chem. A **105**, 10093 (2001).
[36] A. K. Kandalam, B. Kiran, P. Jena, X. Li, A. Grubisic, and K. H. Bowen, J. Chem. Phys. **126**, 084306 (2007).
[37] T. P. Snow, B. L. Rachford, and L. Figorski, Astrophys. J. **573**, 662 (2002).
[38] K. S. De Boer and H. J. G. L. M. Lamers, Astron. Astrophys. **69**, 327 (1978).
[39] B. D. Savage and R. C. Bohlin, Astrophys. J. **229**, 136 (1979).
[40] E. B. Jenkins, B. D. Savage, and L. Spitzer, Astrophys. J. **301**, 355 (1986).
[41] G. Serra, B. Chaudret, Y. Saillard, A. Le Beuze, H. Rabaa, I. Ristorcelli, and A. Klotz, Astron. Astrophys. **260**, 489 (1992).
[42] J. W. Buchanan, J. E. Reddic, G. A. Grieves, and M. A. Duncan, J. Phys. Chem. A **102**, 6390 (1998).
[43] L. Senapati, S. K. Nayak, B. K. Rao, and P. Jena, J. Chem. Phys. **118**,

8671 (2003).
[44] A. Simon and C. Joblin, J. Phys. Chem. A **111**, 9745 (2007).
[45] Y. Wang, J. Szczepanski, and M. Vala, Chem. Phys. **342**, 107 (2007).
[46] M. Gerhards, O. C. Thomas, J. M. Nilles, W.-J. Zheng, and K. H. Bowen, J. Chem. Phys. **116**, 10247 (2002).
[47] A. D. Becke, Phys. Rev. A **38**, 3098 (1988).
[48] J. P. Perdew and Y. Wang, Phys. Rev. B **45**, 13244 (1992).
[49] M. J. Frisch, G. W. Trucks, H. B. Schlegel *et al.*, GAUSSIAN 03, Revision C.02, Gaussian, Inc., Wallingford, CT, 2004.
[50] M. A. Duncan, A. M. Knight, Y. Negishi, S. Nagao, Y. Nakamura, A. Kato, A. Nakajima, and K. Kaya, Chem. Phys. Lett. **309**, 49 (1999).
[51] G. Chen, R. G. Cooks, E. Corpuz, and L. T. Scott, J. Am. Soc. Mass Spectrom. **7**, 619 (1996).
[52] D. G. Leopold and W. C. Lineberger, J. Chem. Phys. **85**, 51 (1986).
[53] F. Liu, S. N. Khanna, and P. Jena, Phys. Rev. B **43**, 8179 (1991).
[54] N. W. Ashcroft and N. D. Mermin, *Solid State Physics* (Holt, Rinehart and Winston, New York, 1976).
[55] C. Kittel, *Introduction to Solid State Physics* (Wiley, New York, 1976).
[56] M. B. Papaconstantanopoulos, *Handbook of the Band Structure of Elemental Solids* (Plenum, New York, 1986), p. 73.
[57] A. Klotz, P. Marty, P. Boissel, D. de Caro, G. Serra, J. Mascetti, P. de Parseval, J. Deroualt, J.-P. Daudey, and B. Chaudret, Planet. Space Sci. **44**, 957 (1996).
[58] B. Chaudret, A. Le Beuze, H. Rabaâ, J. Y. Saillard, and G. Serra, New J. Chem. **15**, 791 (1991).
[59] G. Schmitt, W. Kein, J. Fleischhauer, and U. Walbergs, J. Organomet. Chem. **152**, 315 (1978).
[60] W. H. Morrison, E. Y. Ho, and D. N. Hendrickson, Inorg. Chem. **14**, 500 (1975).
[61] D. Astruc, Tetrahedron **39**, 4027 (1983).
[62] Unpublished results.
[63] G. L. Gutsev and C. W. Bauschlicher, Jr., J. Phys. Chem. A **107**, 7013 (2003).